Draft version January 28, 2020
Typeset using LaTeX **twocolumn** style in AASTeX62_tweeked_for_nat

Progress in unveiling extreme acceleration in persistent astrophysical jets

J. Biteau,[1] E. Prandini,[2] L. Costamante,[3] M. Lemoine,[4] P. Padovani,[5] E. Pueschel,[6] E. Resconi,[7] F. Tavecchio,[8] A. Taylor,[6] and A. Zech[9]

[1]*Institut de Physique Nucléaire d'Orsay (IPNO, now IJC Lab), Université Paris-Sud, Univ. Paris/Saclay, CNRS-IN2P3, France*
[2]*INAF – Osservatorio Astronomico di Padova, Vicolo dell'Osservatorio 3, Padova & Dipartimento di Fisica e Astronomia dell'Università degli Studi di Padova, Padua, Italy*
[3]*ASI – Unità Ricerca Scientifica, Via del Politecnico snc, I-00133, Roma, Italy*
[4]*Institut d'Astrophysique de Paris, CNRS - Sorbonne Université, 98 bis boulevard Arago, F-75014 Paris, France*
[5]*European Southern Observatory, Karl-Schwarzschild-Str. 2, D-85748 Garching bei München, Germany*
[6]*DESY, Platanenallee 6, 15738 Zeuthen, Germany*
[7]*Technische Universität München, Physik-Department, James-Frank-Str. 1, D-85748 Garching bei München, Germany*
[8]*INAF – Osservatorio Astronomico di Brera, via E. Bianchi 46, I-23807, Merate, Italy*
[9]*LUTH, Observatoire de Paris, PSL Research University, CNRS, Université de Paris, 5 Place Jules Janssen, 92190 Meudon, France*

(Dated: August 19, 2019 - submission date)

ABSTRACT

The most powerful persistent accelerators in the Universe are jetted active galaxies. Galaxies whose jets are directed towards Earth, so called blazars, dominate the extragalactic γ-ray sky. Still, most of the highest-energy accelerators likely elude detection. These extreme blazars, whose radiated energy can peak beyond 10 TeV, are ideal targets to study particle acceleration and radiative processes, and may provide links to cosmic rays and astrophysical neutrinos. The growing number of extreme blazars observed at TeV energies has been critical for the emergence of γ-ray cosmology, including measurements of the extragalactic background light, tight bounds on the intergalactic magnetic field, and constraints on exotic physics at energies inaccessible with human-made accelerators. Tremendous progress is expected in the decade to come, particularly with the deployment of the Cherenkov Telescope Array.

Keywords: acceleration of particles; astroparticle physics; cosmology: diffuse radiation; galaxies: jets; radiation mechanisms: non-thermal

1. INTRODUCTION

The luminosity of most galaxies is dominated by thermal emission from stars. For the remaining $\gtrsim 1\%$, emission from the active galactic nucleus (AGN), which hosts a super-massive black hole ($10^6 - 10^{10}\,M_\odot$), can completely outshine the billions of stars in the galaxy [1]. Up to $\sim 10\%$ of AGN develop two-sided relativistic jets that emit non-thermally over the whole electromagnetic spectrum [2]. The emitting region in the jet moves away from the super-massive black hole with a relativistic bulk velocity that, for small viewing angles ($\theta < 10 - 15°$), Doppler shifts the luminosity of the source to higher frequencies by a factor $\delta_{\rm D} = \mathcal{O}(10)$, and amplifies the bolometric emission by $\delta_{\rm D}^4$. Such an AGN is called a blazar.

The broad-band spectral energy distribution (SED) of blazars is characterized by two distinctive humps. The first hump, peaking at infrared to X-ray wavelengths, is commonly explained as synchrotron emission from electrons accelerated in the jet. The second hump, peaking above MeV energies, is often attributed to inverse-Compton scattering, possibly of the same electrons on their own synchrotron emission (synchrotron self-Compton model, SSC). Blazars form a continuous sequence from low- to high-energy peaked objects, with an overall correlation of the frequencies of the two peaks. The end of the sequence is dominated by high-frequency-peaked BL Lac objects (HBL, [3]), *i.e.*, blazars with weak emission lines and radiatively inefficient accretion disks. HBLs are characterized by synchrotron emission peaking at $\bar{\nu}_{\rm x} \gtrsim 10^{15}$ Hz (~ 4 eV), with the most *extreme blazars* showing larger values by at least two orders of magnitude [4].

No other persistent engine in the Universe generates as much power beyond TeV energies as extreme blazars. A coherent description of their neutral radiation (photons and possibly neutrinos) and of the hadronic/leptonic content of their jets constitutes a challenge for current models [5].

A fraction of the γ-rays emitted by extreme blazars at TeV energies is absorbed before reaching the observer. This leaves a spectral imprint that is exploited to measure the extragalactic background light (EBL), to constrain electromagnetic cascades within the intergalactic magnetic field (IGMF), and to probe exotic physics [6].

This review aims to offer a comprehensive view of extreme blazars, connecting recent advances in the astrophysics, astroparticle, and fundamental physics communities.

2. EXTREME OBSERVATIONAL PROPERTIES

2.1. *Multi-wavelength observations of extreme blazars*

Extreme blazars come in two flavours: *extreme-synchrotron* sources show a synchrotron peak energy $h\bar{\nu}_{\rm x} \geq 1\,{\rm keV}$ (2.4×10^{17} Hz); *extreme-TeV* sources have a γ-ray peak energy $h\bar{\nu}_\gamma \geq 1\,{\rm TeV}$ (2.4×10^{26} Hz) (*e.g.*, [7, 8]). This is revealed by a hard spectrum in the soft X-ray band $\Gamma_{\rm x} < 2$, or in the $0.1-1$ TeV band, $\Gamma_\gamma < 2$. The intrinsic spectrum is recovered from the observed spectrum by accounting for absorption, namely photoelectric absorption in intervening gas for X-rays and γ-EBL interactions at GeV-TeV energies (see Sec. 4.1).

In the optical band, measurements of the flux and polarization of extreme blazars are generally dominated by the thermal emission of the giant elliptical host galaxy. These sources show radio properties similar to other HBLs, but their flux is generally very low. Indeed, a high X-ray to radio flux ratio is a very effective way to select *extreme-synchrotron* sources among normal HBLs (see Sec. 2.2). The combination of an *extreme-synchrotron* nature with a hard GeV flux appears to be a multi-wavelength marker favoring the selection of *extreme-TeV* sources.

Extreme blazars were discovered in 1996-97, with *Beppo*SAX observations of flares from Mkn 501 [9] and 1ES 2344+514 [10]. Mkn 501 reached synchrotron peak frequencies $h\bar{\nu}_{\rm x} > 100\,{\rm keV}$, with an increase of the luminosity by a factor of 20 in a few days and a typical "harder-when-brighter" behaviour (Fig. 1, left). *Beppo*SAX also discovered in 1999 the first example of extreme source in low or quiescent state, with 1ES 1426+428 displaying a hard and straight power-law spectrum over three decades in energy [7]. With observed $h\bar{\nu}_{\rm x} \gtrsim 100\,{\rm keV}$, Mkn 501 and 1ES 1426+428 can be considered prototypical of the *extreme-synchrotron* subclass.

The first *extreme-TeV* blazars were discovered in 2006 with H.E.S.S. [17]. The intrinsic spectra of 1ES 1101-232 and H 2356+304 were unusually hard even after accounting for absorption with the lowest possible EBL intensity, locating the γ-ray peak definitively above $1-3$ TeV. With the present knowledge of the EBL, eleven blazars with measured redshift can be classified as *extreme-TeV* objects (see Table 1 and TeVCat [18]). Three other blazars have shown *extreme-TeV* properties but only temporarily, namely Mkn 501, 1ES 1727+502, and 1ES 1426+428. *Extreme-TeV* properties were also found in IC 310, a peculiar nearby AGN ($z = 0.0189$) whose jet might be misaligned by $10-20^\circ$ from the line of sight [19]. The record for the highest γ-ray peak energy observed is held by the prototypical *extreme-TeV* blazar 1ES 0229+200 (see Fig. 1), with $h\bar{\nu}_\gamma \gtrsim 10\,{\rm TeV}$ and an intrinsic spectrum with $\Gamma_\gamma \simeq 1.5$ [20].

Most *extreme-TeV* sources appear steady over years at TeV energies, although large statistical uncertainties make it difficult to rule out flux variations such as seen in X-rays over similar timespans. The only firm evidence was found in 1ES 1218+304, with a fast flare over a few days reaching $\sim20\%$ of the Crab nebula flux [21]. There are indications of a factor of $2-3$ variations in 1ES 0229+200 on year timescales [22]. In both cases, the TeV spectrum remained hard, indicating no change in the *extreme-TeV* character of these objects. On the contrary, during a long active phase in 2012, Mkn 501 showed both synchrotron and γ-ray peaks shifted from normal to extreme energies, by ~3 and ~1 decade in energy respectively [23]. The synchrotron peak of 1ES 1727+502 similarly shifted between 2011 and 2013 [24].

The relationship between *extreme-synchrotron* and *extreme-TeV* blazars is not established. There are 24 extreme blazars with firm redshift and published TeV spectrum (see Table 1). Twenty three of these are *extreme-synchrotron* sources, at least half of which (13/23) are also *extreme-TeV* blazars. On the other hand, thirteen of the fourteen known *extreme-TeV* blazars are also *extreme-synchrotron* in same-epoch observations or in other epochs. This suggests that *extreme-TeV* sources may have a greater tendency to display *extreme-synchrotron* behaviour at some point in their emission history than the reverse scenario.

As illustrated in Fig. 1, the emerging picture is that there are three distinct extreme behaviours:

1. becoming extreme during large flares, when both peaks shift to higher energies (Mkn 501-like). These objects revert back to their standard HBL state;

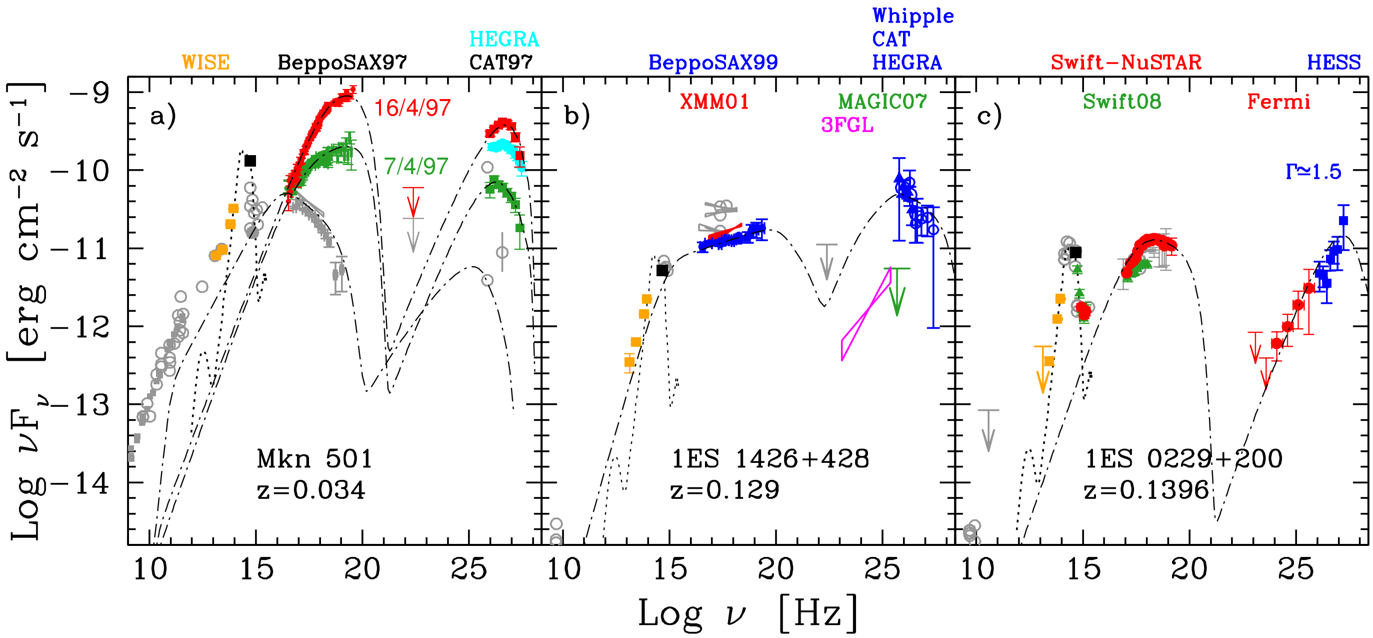

Figure 1. Prototypical SEDs showing the three types of extreme behaviours: *extreme-synchrotron*, either during short-lived large flares and long-lasting quiescent states (panels a and b) and *extreme-TeV* (panel c). Observed γ-ray spectra are corrected for EBL absorption [11]. Historical data taken close to the same epoch are shown with the same colour and labelled accordingly. Grey points correspond to archival data. Dash-dotted lines show SSC models and are reported as guidelines. Dotted lines show the host-galaxy emission, using the template spectrum of a giant elliptical galaxy [12], scaled to match the magnitude of the host galaxy [13]. Data and models are from [9, 14, 15] for Mkn 501, [16] for 1ES 1426+428 and [8] for 1ES 0229+200.

2. showing a steady, hard synchrotron spectrum up to $10-100$ keV (1ES 1426+428-like), which is not accompanied by a hard TeV spectrum;
3. showing a persistently hard γ-ray spectrum with a peak above several TeV, which remains mostly unchanged across flux variations (1ES 0229+200-like). Their synchrotron spectrum tends to peak in the X-ray band.

2.2. *Catalogues and population studies*

Population studies of extreme blazars are currently restricted to the *extreme-synchrotron* subclass, due to the lack of an unbiased extragalactic survey at TeV energies.

The largest catalogue of extreme blazars to date is the 3HSP, which builds on the 1WHSP and the 2WHSP (see [25] and references therein). The 1WHSP catalogue assembled a large sample of HBLs starting from the ALLWISE infrared survey and applying further restrictions on their infrared slope, as well as on their infrared/radio and infrared/X-ray flux ratios. The 2WHSP abandoned the infrared slope criterion, as it excluded sources dominated by the host galaxy. The 3HSP catalogue complemented the 2WHSP sample with *Fermi*-LAT γ-ray sources with hard spectra ($\Gamma_\gamma < 2$) and with objects with a high X-ray to radio flux ratio, thus selecting HBLs. The final sample includes 2,011 HBLs, with redshift information for 88% of them (including photometric estimates), out of which 199 qualify as *extreme-synchrotron* blazars. All presently known *extreme-TeV* blazars are part of the 3HSP.

The 3HSP catalogue is flux-limited in the radio and X-ray bands for sources with $\bar{\nu}_{\rm x} > 10^{16}$ Hz. Radio num-

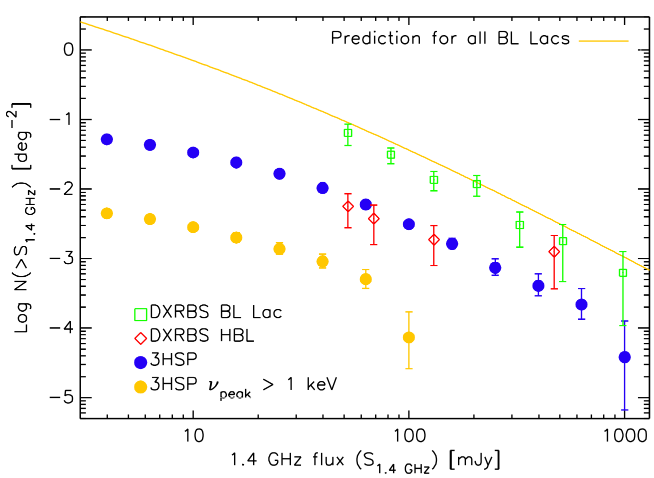

Figure 2. Radio number counts of different samples of BL Lacs. Green squares denote Deep X-Ray Radio Blazar Survey (DXRBS) BL Lacs, red trapezoids DXRBS HBLs, blue circles the 3HSP sample, and orange circles the extreme 3HSP blazars. The solid line represents the predicted number counts based on the luminosity function of [2]. Figure adapted from [25], courtesy of Yu-Ling Chang.

ber counts are displayed in Fig. 2, together with the number counts of other BL Lac samples from the Deep X-ray Radio Blazar Survey [26]. The slopes of the subsample distributions are similar, implying that the fraction of high-$\bar{\nu}_{\rm x}$ blazars is roughly independent of radio flux. *Extreme-synchrotron* blazars represent about 10% of HBLs, which in turn correspond to 10% of all BL Lacs.

Above a radio flux of 3.5 mJy at 1.4 GHz, the surface density of $\sim 4.5 \times 10^{-3}$ deg^{-2} inferred for extreme blazars corresponds to a total number of *extreme-synchrotron* sources over the sky of ~ 200. The maximum observed radio luminosity tends to be lower for extreme blazars than for regular HBLs. This is consistent with the inferred anti-correlation between power and $\bar{\nu}$ often denoted as the "blazar sequence" [27], which can also be explained by selection effects [28]. The rareness of *extreme-synchrotron* sources suggests the latter, as these sources, which are at the low end of the luminosity function, would be expected to represent the most common subclass along the blazar sequence.

3. THE CHALLENGE OF MODELING EXTREME BLAZARS

The simplest one-zone SSC models generally represent well the stationary SED of most HBLs with $h\bar{\nu}_\gamma < 1$ TeV, including purely *extreme-synchrotron* sources. This suggests that *extreme-synchrotron* sources are the high-energy tail of the blazar population. On the other hand, the origin of the *extreme-TeV* emission is still unknown, and with the attributes of the sources. *Extreme-TeV* blazars present two essential challenges:

1. explaining the peak of radiation at TeV energies: $h\bar{\nu}_\gamma > 1$ TeV.

2. explaining the hard intrinsic spectrum of the component radiated at sub-TeV energies: $\Gamma_\gamma < 2$.

A hard intrinsic spectrum at TeV energies, $F_\nu/\nu \propto \nu^{-\Gamma_\gamma}$ with $\Gamma_\gamma \simeq 1.5$, typically implies a hard accelerated particle spectrum, $\mathrm{d}N/\mathrm{d}\gamma \propto \gamma^{-p}$ with $p < 2$, so that most of the energy is carried by the highest-energy particles, an unusual case in astrophysics. The spectral index derives from a competition between energy gains and escape or energy losses in the acceleration region. The universal relationship between energy gain and escape in shock acceleration implies an index $p \geq 2$ (see *e.g.*, [29]). In more involved configurations that either decrease the escape probability or increase the energy gain, harder spectra remain possible (*e.g.*, [30]). There is no generic prediction for acceleration in magnetized turbulence or in reconnection outflows, and both hard and soft particle spectra appear to be possible [31].

The observations of most blazars are matched by phenomenological models, which leave the acceleration scenario unspecified and fit the environmental parameters and the accelerated particle spectrum to reproduce SEDs. These models are separated into two classes: leptonic for electrons and positrons, hadronic for protons and nuclei.

3.1. *Leptonic scenarios*

In simple one-zone SSC models, TeV radiation results from inverse-Compton scattering of electrons or pairs with comoving-frame energy ϵ'_e. A peak emission beyond 1 TeV imposes $\delta_{\rm D}\,\epsilon'_e > 1$ TeV in the Klein-Nishina regime, which implies high Lorentz factors for the electrons, $\gamma'_e = \epsilon'_e/m_e c^2 > 2{\times}10^5 \times (\delta_{\rm D}/10)^{-1}$. Both the high $\bar{\nu}_\gamma$ and hard Γ_γ of *extreme-TeV* blazars are matched by such models provided the electron distribution shows a minimum Lorentz factor with a sufficiently large value, sometimes up to $\gamma_{\rm min} \simeq 10^4 - 10^5$ (*e.g.*, [32]). This requires an unusually low radiative efficiency and conditions out of equipartition by several orders of magnitude. A sub-TeV spectrum as hard as $\Gamma_\gamma = 2/3$ can be obtained in a weakly magnetized environment ($B \lesssim 1$ mG) where spectral softening due to synchrotron cooling is reduced.

A different approach within the leptonic framework considers additional inverse-Compton components from external photon fields. Models with a sheath surrounding an inner jet [33] struggle to reproduce a high $\bar{\nu}_\gamma$, due to the intense target photon field. However, upscattering of photons from the broad-line region in a compact emission zone [34] or of cosmic microwave background (CMB) photons in the extended kpc-jet [35] could reproduce a hard emission spectrum up to TeV energies. These scenarios require either a sufficiently luminous broad-line region, which is not usually expected for extreme blazars and other BL Lacs, or a very energetic particle distribution over kpc scales. The latter would lead to steady TeV emission over thousands of years, in contradiction with flux variations detected in 1ES 1218+304.

The most successful leptonic models applied to *extreme-TeV* blazars thus appear to be simple SSC models including $\gamma_{\rm min} \gg 1$ or steep particle spectra. As an example, the model for 1ES 0229+200 in Fig. 1 and Fig. 3 assumes a moderate $\gamma_{\rm min} = 100$, a very steep particle spectrum with index $p = 1.4$, a high Doppler factor $\delta_D = 50$ and a low magnetic field of 2 mG. The electron energy density dominates over the magnetic one by a factor of $\sim 10^5$.

The requirement of weak magnetization appears to disfavour reconnection scenarios, which could nonethe-

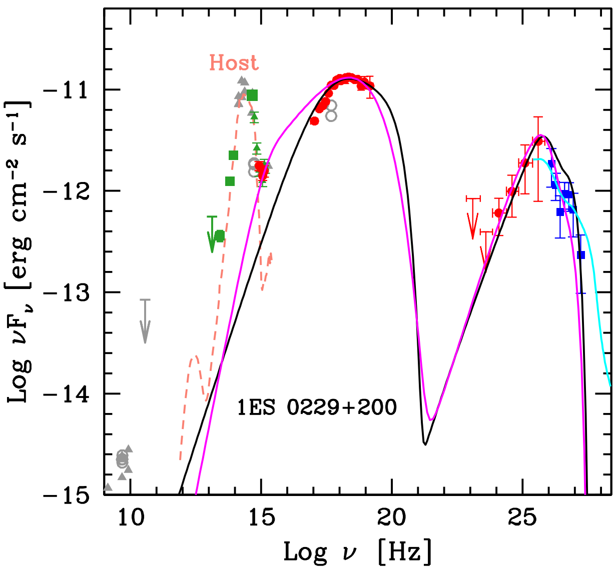

Figure 3. Leptonic SSC model (black line, from [8]), proton synchrotron model (magenta, adapted from [38]) and external cascade model (cyan, from [39], covering only the γ-ray range) of the observed SED of 1ES 0229+200. γ-ray data are *not* corrected for EBL absorption. The orange dashed line shows the emission from the host galaxy.

less produce high $\gamma_{\rm min}$ values (*e.g.*, [36]). Stochastic acceleration could result in narrow pseudo-Maxwellian particle distributions with high peak energies, irrespective of the magnetization level (*e.g.*, [37]). However, pushing electrons from mildly relativistic energies up to $\gamma_{\rm min}$ necessitates an energy reservoir that is initially $\gamma_{\rm min}$ larger than the particle energy content, which implies a high jet power.

3.2. *(Lepto-)hadronic models*

Typical hadronic scenarios are based on the co-acceleration of protons and electrons and attribute the TeV emission to proton synchrotron radiation, possibly mixed with SSC emission from secondary pairs (*e.g.*, [38]). Proton synchrotron scenarios require ultra-high-energy particles with $\epsilon'_p > 10^{19}\,{\rm eV} \times (B'/100\,{\rm G})^{-1/2}$ in a strong comoving-frame magnetic field, B' [40]. Mixed models propose instead an energy budget dominated by the kinetic energy of protons. Such models require hard particle injection spectra, with p from 1.3 to 1.7, as well as large jet energetics, typically close to the Eddington limit of the central black hole.

If extreme blazars accelerate very-high-energy cosmic rays, the observed TeV emission might even result from secondary radiation produced outside the source, through an electromagnetic cascade triggered by photo-pion or photo-pair production on the EBL and CMB (*e.g.*, [39, 41–43]). The original version of this scenario assumed protons or nuclei with energies $\sim 10^{16}$ eV, well below the ankle of the UHECR spectrum (at a few 10^{18} eV). However, nuclei are deflected by magnetic fields associated to structures of the cosmic web (voids, clusters, filaments, with magnetic fields up to 10 nG), which broadens the beam and increases the luminosity required to reproduce the observed γ-ray spectra [44]. Such models predict slower variability than that observed, although synchrotron radiation from secondary pairs in magnetic fields extending on Mpc scales could account for variability down to year timescales [45].

As an example, Fig. 3 shows a one-zone proton synchrotron model and an external cascade model applied to 1ES 0229+200. The proton synchrotron model requires a much larger magnetic field ($B' \simeq 20$ G) than the leptonic model, comparable values for $\gamma_{\rm min} \simeq 100$ and the Doppler factor, $\delta_{\rm D} \simeq 30$. The particle spectra are again very steep and the considerable energy of the protons leads to a jet power at the Eddington limit.

This expository proton synchrotron model predicts a peak neutrino flux of $\sim 10^{-15}\,{\rm erg\,cm^{-2}\,s^{-1}}$ around 10^{19} eV. Such fluxes are beyond the reach of current-generation neutrino observatories. On the other hand, the recent indication of a link between a neutrino track event and TXS 0506+056 [46, 47], which is a regular BL Lac, can be successfully modelled if a sub-dominant component of the γ-ray emission arises instead from $p\gamma$ or pp interactions [48–51]. These two hadronic channels are not expected to dominate the emission of *extreme-TeV* blazars, but the rest of the blazar population of the blazar population have been proposed to contribute to the neutrino and cosmic-ray background up to the ankle (*e.g.*, [52, 53]).

Above the ankle, the phenomenological modelling of the UHECR spectrum and composition observables suggests particle spectra as hard as $p < 1$ escaping from the sources [54]. Solutions with $p \simeq 1.5 - 2$ are obtained for source populations with a negative evolution [55], as inferred for HBLs and in particular extreme blazars [25, 56].

At even higher energies, close to 10^{20} eV, interactions with the EBL and the CMB constrain the nearest UHECR sources to lie strictly within 100 Mpc [57, 58]. Although the nearest extreme blazar, Mkn 501, is at a luminosity distance of ~ 150 Mpc, misaligned counterparts could satisfy the local proximity constraint. Because of a tight lower bound on the magnetic luminosity (*e.g.*, [59]), only the most luminous sources should be able to reach the highest energies, so that nearby ones could already be identified in electromagnetic surveys [60].

Whether AGN jets can accelerate UHECRs remains unresolved. Neglecting energy losses, the maximum energy [57] can be estimated by balancing the acceleration timescale, $t_{\rm acc}$, with the escape timescale. The ratio $t_{\rm acc}/t_{\rm L}$, where $t_{\rm L}$ is the Larmor or gyration time, is constrained by the peak synchrotron frequency in the comoving frame, as $t_{\rm acc}/t_{\rm L} \lesssim 150\,{\rm MeV}/h\bar{\nu}'_{\rm x}$ [61, 62]. The high $\bar{\nu}_{\rm x}$ of extreme sources suggests that they are the fastest and thus the most efficient accelerators of the AGN population.

4. EXTREME BLAZARS AND TESTS OF γ-RAY PROPAGATION

4.1. *Cosmology: Extragalactic Background Light*

The γ-ray spectra of blazars are softened by pair-production interactions with the EBL above $\sim$100 GeV, in an energy- and redshift-dependent fashion shown in Fig. 4 (*e.g.*, [63]). The first component of EBL, peaking at optical frequencies, is now well determined thanks to both direct modeling (*e.g.*, [11]) and γ-ray constraints (*e.g.*, [6, 64]). Emission from *extreme-TeV* blazars detected around 10 TeV provides constraints on the EBL intensity up to $\sim 50\,\mu$m. The limited number of *extreme-TeV* sources has thus left the second hump of the EBL (mid- to far-infrared) poorly constrained.

EBL measurements based on blazars with a firm redshift rely on assumptions about the intrinsic emission prior to absorption. In the absence of full SED modelling, intrinsic spectra are assumed to be well-described by power-law or log-parabola functions with the flux decreasing at the highest energies. The absence of strong broad-line regions in extreme blazars supports these assumptions: internal absorption, which can lead to upturns or EBL-mimicking spectral feature, is expected and observed to be minimal.

A major step forward came with the H.E.S.S. spectral measurements of 1ES 1101-232 and H 2356+304 in 2006 [17]. Their hard spectra provided the first strong constraints to the maximum intensity of the EBL. Current TeV measurements rely on observations of both steady and temporary *extreme-TeV* blazars to constrain the longest wavelengths [65, 66].

4.2. *Cosmology: Intergalactic Magnetic Field*

With their hard and high-energy emission, *extreme-TeV* blazars offer a unique possibility to constrain the presence of cascades in the IGMF. The strength of the IGMF is not well constrained, despite its relevance ([69] for a review). It may have provided the seed field for magnetic fields in galaxies and galaxy clusters, and measurement of its strength and correlation length could distinguish between generation scenarios (in the early Universe or after the formation of the first galaxies).

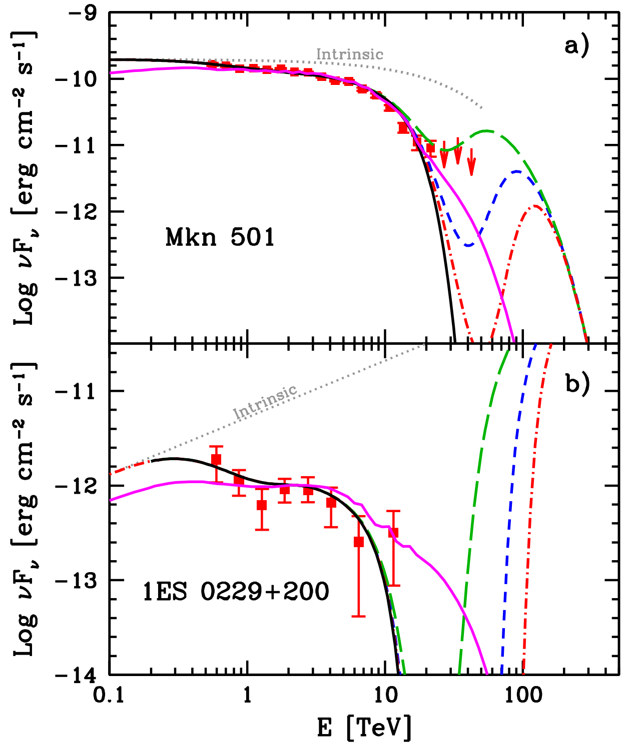

Figure 4. Models of the observed γ-ray spectra of the extreme blazars 1ES 0229+200 [20] and Mkn 501 (during its active phase in 1997, [14]). γ-ray data are *not* corrected for EBL absorption. The solid black line shows the expected spectra after interaction with the EBL, assuming the intrinsic emission shown by the dotted grey line. The modifications induced by Lorentz invariance violation [67] are shown by the long-dashed green, dashed blue and dash-dotted red lines for $E_{\rm LIV} = 3\times10^{19}$, 10^{20} and 2×10^{20} GeV, respectively. The magenta solid line shows the spectrum modified by mixing with axion-like particle [68].

An electromagnetic cascade develops when electron-positron pairs generated by γ-EBL interactions upscatter CMB photons to GeV energies. All the energy flux absorbed at TeV energies is reprocessed into the GeV band. The cascade develops when inverse-Compton scattering proceeds faster than plasma cooling of the pair beam. The relative cooling speeds depend on the primary γ-ray spectrum, Γ_γ [70]. The deflection of electrons and positrons in the IGMF angularly broadens the cascade and introduces a time delay with respect to primary γ-rays, thereby affecting the low-energy γ-ray component.

Spectral observations in the GeV-TeV range constrain the strength of the IGMF to be larger than a few femto-Gauss, while searches for angular broadening have constrained intervals of even higher magnetic field [71–73]. The predicted cascade component at GeV energies is particularly large for extreme blazars, due to their hard intrinsic spectra, and to the relative stability of their flux, which reduces uncertainties introduced by arrival-time delays. The strongest individual lower limits from *Fermi*-LAT come from 1ES 0229+200 and 1ES 0347-121, while the VERITAS and H.E.S.S. exclusion regions make use of observations of 1ES 1218+304, 1ES 1101-232 and 1ES 0229+200.

4.3. *Fundamental physics*

Due to their emission at multi-TeV energies, extreme blazars are considered prime candidates for the search for spectral anomalies in the TeV spectra, as theorized for Lorentz invariance violation [74] or mixing with axion-like particles [75].

Phenomenologically, Lorentz invariance violation leads to modifications of the dispersion relations of particles and photons, implying in particular the alteration of the pair production threshold above a γ-ray energy $E_{\rm mod} \simeq [(2m_e c^2)^2 E_{\rm LIV}^n/(1-2^{-n})]^{1/(n+2)}$, where n is the order of the correction and $E_{\rm LIV}$ is the energy scale at which Lorentz invariance is violated [6]. Above $E_{\rm mod}$, pair production is virtually forbidden and the Universe becomes transparent. Limits coming from present measurements, including the complementary approach based on time-of-flight, constrain $E_{\rm LIV}$ to be above the Planck scale (1.2×10^{19} GeV) for $n = 1$ [76], indicating that effects would potentially be detectable only above $E_{\rm mod} \simeq 50$ TeV. The best prospects are probably offered by the very-high states of Mkn 501, such as those displayed during 1997 and 2014 [14, 77].

Axion-like particles are generically predicted by several extensions of the Standard Model (such as string theory). They are expected to be light, neutral, and to couple to two photons, implying conversion of γ-rays to axion-like particles in a magnetic field. The particle-photon oscillation during propagation could lead to ripples in the γ-ray spectra [78] and to a substantial reduction of the effective opacity at the highest energies [75], as illustrated in Fig. 4. For moderate redshifts, the reduction of the opacity is particularly relevant above few TeV. *Extreme-TeV* blazars are therefore natural candidates for these studies [68].

5. PERSPECTIVES

Three main research lines should guide future observations of extreme blazars: (i) population studies, featuring the characterization of a large number of extreme blazars at TeV energies; (ii) emission mechanisms, including the measurement of variability timescales in the TeV band; (iii) jet hadronic content, connecting extreme blazars and multi-messenger observations.

The current knowledge of the extreme-blazar population is based on surveys from radio wavelengths to X-rays. eROSITA will further enlarge the *extreme-synchrotron* population with the first imaging all-sky survey up to 10 keV [79]. IXPE will open the X-ray polarimetric window, probing the magnetic fields and jet content of extreme blazars [80]. At higher energies, future MeV telescopes such as AMEGO and e-ASTROGAM (*e.g.*, [81]) have the potential to observe the high end of the *extreme-synchrotron* population.

As the next-generation γ-ray observatory, the Cherenkov Telescope Array (CTA, [82]) will play a central role in establishing a census of *extreme-TeV* sources. Thanks to its sensitivity, CTA will likely discover numerous extremely hard objects, too faint to be detected with *Fermi*-LAT and current TeV instruments. The CTA survey of a quarter of the extragalactic sky, complemented in the multi-TeV range by LHAASO [83] and SWGO [84], will provide for the first time an unbiased view on the *extreme-TeV* population, blazars and their off-axis counterparts. This latter subclass of radio galaxies constitutes a promising field of research both for AGN population studies and for the search of the origin of UHECRs.

The physics of particle acceleration in extreme environments has benefited from the emergence of *ab initio* numerical simulations that focus on the microscopic scales of acceleration, at the expense of idealizing on macroscopic scales (see [29, 31, 85] for recent advances). Conversely, phenomenological modeling often integrates out the microphysics to deal with the macroscopic scales of the source. A major challenge of the coming years lies in bridging this gap, including *e.g.*, a realistic description of relativistic jets and of their environment, as well as propagation in intervening magnetic and photon fields. In particular, an improved knowledge of the IGMF would benefit both the study of cosmic-ray sources and tests of external cascade scenarios.

A productive interplay between theory, phenomenology and observations will be fostered by the broad-range measurements from $\sim$30 GeV to hundreds TeV offered by CTA. The improved sensitivity with respect to current-generation instruments by a factor of $5-20$ depending on energy will make it possible to test emission and propagation models with unprecedented accuracy. With the long-term monitoring program of CTA dedicated to AGN, we expect to access for the first time to time-resolved, broad γ-ray spectra of *extreme-TeV* blazars. TeV observations will be complemented by X-ray monitoring with *Swift*-XRT and future satellites like SVOM [86].

As very-high-energy extragalactic accelerators, extreme blazars are prime candidates to investigate multi-messenger correlations with neutrinos and cosmic rays. Significant improvements in the statistics of these astroparticles and in their composition are expected from next-generation astroparticle observatories, including IceCube-Gen2 [87], KM3NeT [88], for the neutrino sector, and AugerPrime [89] and TA×4 [90] for the cosmic-ray sector. The detection of astroparticle flux excesses associated with electromagnetic sources remains a most promising avenue to understand acceleration, radiative and escape mechanisms at energies beyond the reach of human-made accelerators.

This review is the result of several fruitful discussions raised during the meeting *eXtreme19* (22-25 January 2019, Padova, Italy). The authors, as chairs of the scientific committee and review speakers, wish to thank all the participants to the meeting: C. Arcaro, B. Balmaverde, U. Barres de Almeida, E. Benítez, D. Bernard, E. Bernardini, M. Boettcher, S. Boula, A. Caccianiga, C. Casadio, I. Christie, A. De Angelis, L. Di Gesu, A. di Matteo, I. Donnarumma, M. Doro, T. Dzhatdoev, V. Fallah Ramazani, R. Ferrazzoli, I. Florou, L. Foffano, L. Foschini, N. I. Fraija, A. Franceschini, G. Galanti, M. Gonzalez, O. Gueta, O. Hervet, S. Kerasioti, F. Krauss, M. Kreter, G. La Mura, R. Lico, R. Lopez Coto, M. Lucchini, M. Mallamaci, M. Manganaro, A. Marinelli, M. Mariotti, K. Nalewajko, E. Nokhrina, F. Oikonomou, L. Olivera-Nieto, S. Paiano, V. Paliya, D. Paneque, Z. Pei, C. Perennes, S. Rainò, P. Romano, A. Sharma, G. Sigl, C. Sinnis, P. Soffitta, A. Spolon, B. Sversut Arsioli, A. Tramacere, S. Vercellone, V. Vittorini, and H. Xiao.

EPr has received funding from the European Union's Horizon2020 research and innovation programme under the Marie Sklodowska–Curie grant agreement no 664931. EPu acknowledges the Young Investigators Program of the Helmholtz Association. FT acknowledges contribution from the grant INAF CTA–SKA "Probing particle acceleration and γ-ray propagation with CTA and its precursors" and the INAF Main Stream project "High-energy extragalactic astrophysics: toward the Cherenkov Telescope Array".

REFERENCES

[1] Padovani, P. *et al.* Active galactic nuclei: what's in a name? *Astron. Astrophys Rev.* **25**, 2 (2017).

[2] Urry, C. M. & Padovani, P. Unified Schemes for Radio-Loud Active Galactic Nuclei. *Publ. Astron. Soc. Pac.* **107**, 803 (1995).

[3] Padovani, P. & Giommi, P. The connection between x-ray- and radio-selected BL Lacertae objects. *Astrophys. J.* **444**, 567–581 (1995).

[4] Ghisellini, G. Extreme blazars. *Astropart. Phys.* **11**, 11–18 (1999).

[5] Böttcher, M. Progress in Multi-wavelength and Multi-Messenger Observations of Blazars and Theoretical Challenges. *Galaxies* **7**, 20 (2019).

[6] Biteau, J. & Williams, D. A. The Extragalactic Background Light, the Hubble Constant, and Anomalies: Conclusions from 20 Years of TeV Gamma-ray Observations. *Astrophys. J.* **812**, 60 (2015).

[7] Costamante, L. *et al.* Extreme synchrotron BL Lac objects. Stretching the blazar sequence. *Astron. Astrophys.* **371**, 512–526 (2001).

[8] Costamante, L. *et al.* The NuSTAR view on hard-TeV BL Lacs. *Mon. Not. R. Astron. Soc.* **477**, 4257–4268 (2018).

[9] Pian, E. *et al.* BeppoSAX Observations of Unprecedented Synchrotron Activity in the BL Lacertae Object Markarian 501. *Astrophys. J. Lett.* **492**, L17 (1998).

[10] Giommi, P., Padovani, P. & Perlman, E. Detection of exceptional X-ray spectral variability in the TeV BL Lac 1ES 2344+514. *Mon. Not. R. Astron. Soc.* **317**, 743–749 (2000).

[11] Franceschini, A. & Rodighiero, G. The extragalactic background light revisited and the cosmic photon-photon opacity. *Astron. Astrophys.* **603**, A34 (2017).

[12] Silva, L., Granato, G. L., Bressan, A. & Danese, L. Modeling the Effects of Dust on Galactic Spectral Energy Distributions from the Ultraviolet to the Millimeter Band. *Astrophys. J.* **509**, 103–117 (1998).

[13] Scarpa, R. *et al.* The Hubble Space Telescope Survey of BL Lacertae Objects. I. Surface Brightness Profiles, Magnitudes, and Radii of Host Galaxies. *Astrophys. J.* **532**, 740–815 (2000).

[14] Aharonian, F. A. *et al.* The time averaged TeV energy spectrum of MKN 501 of the extraordinary 1997 outburst as measured with the stereoscopic Cherenkov telescope system of HEGRA. *Astron. Astrophys.* **349**, 11–28 (1999).

[15] Tavecchio, F. *et al.* Theoretical Implications from the Spectral Evolution of Markarian 501 Observed with BeppoSAX. *Astrophys. J.* **554**, 725–733 (2001).

[16]Ghisellini, G., Celotti, A. & Costamante, L. Low power BL Lacertae objects and the blazar sequence. Clues on the particle acceleration process. *Astron. Astrophys.* **386**, 833–842 (2002).

[17]Aharonian, F. *et al.* A low level of extragalactic background light as revealed by γ-rays from blazars. *Nature* **440**, 1018–1021 (2006).

[18]Wakely, S. P. & Horan, D. TeVCat: An online catalog for Very High Energy Gamma-Ray Astronomy. *ICRC* **3**, 1341–1344 (2008).

[19]Ahnen, M. L. *et al.* First multi-wavelength campaign on the gamma-ray-loud active galaxy IC 310. *Astron. Astrophys.* **603**, A25 (2017).

[20]Aharonian, F. *et al.* New constraints on the mid-IR EBL from the HESS discovery of VHE γ-rays from 1ES 0229+200. *Astron. Astrophys.* **475**, L9–L13 (2007).

[21]Acciari, V. A. *et al.* Discovery of Variability in the Very High Energy γ-Ray Emission of 1ES 1218+304 with VERITAS. *Astrophys. J.* **709**, L163–L167 (2010).

[22]Aliu, E. *et al.* A Three-year Multi-wavelength Study of the Very-high-energy γ-Ray Blazar 1ES 0229+200. *Astrophys. J.* **782**, 13 (2014).

[23]Ahnen, M. L. *et al.* Extreme HBL behavior of Markarian 501 during 2012. *Astron. Astrophys.* **620**, A181 (2018).

[24]Archambault, S. *et al.* VERITAS Detection of γ-Ray Flaring Activity From the BL Lac Object 1ES 1727+502 During Bright Moonlight Observations. *Astrophys. J.* **808**, 110 (2015).

[25]Chang, Y.-L., Arsioli, B., Giommi, P., Padovani, P. & Brandt, C. The 3HSP catalogue of Extreme High Synchrotron Peaked Blazars. *Astron. Astrophys. in press, arXiv:1909.08279* (2019).

[26]Padovani, P., Giommi, P., Landt, H. & Perlman, E. S. The Deep X-Ray Radio Blazar Survey. III. Radio Number Counts, Evolutionary Properties, and Luminosity Function of Blazars. *Astrophys. J.* **662**, 182–198 (2007).

[27]Ghisellini, G., Righi, C., Costamante, L. & Tavecchio, F. The Fermi blazar sequence. *Mon. Not. R. Astron. Soc.* **469**, 255–266 (2017).

[28]Giommi, P. *et al.* A simplified view of blazars: clearing the fog around long-standing selection effects. *Mon. Not. R. Astron. Soc.* **420**, 2899–2911 (2012).

[29]Sironi, L., Keshet, U. & Lemoine, M. Relativistic Shocks: Particle Acceleration and Magnetization. *Space Sci. Rev.* **191**, 519–544 (2015).

[30]Bykov, A. M., Gladilin, P. E. & Osipov, S. M. Non-linear model of particle acceleration at colliding shock flows. *Mon. Not. R. Astron. Soc.* **429**, 2755–2762 (2013).

[31]Kagan, D., Sironi, L., Cerutti, B. & Giannios, D. Relativistic Magnetic Reconnection in Pair Plasmas and Its Astrophysical Applications. *Space Sci. Rev.* **191**, 545–573 (2015).

[32]Katarzyński, K., Ghisellini, G., Tavecchio, F., Gracia, J. & Maraschi, L. Hard TeV spectra of blazars and the constraints to the infrared intergalactic background. *Mon. Not. R. Astron. Soc.* **368**, L52–L56 (2006).

[33]Chhotray, A. *et al.* On radiative acceleration in spine-sheath structured blazar jets. *Mon. Not. R. Astron. Soc.* **466**, 3544–3557 (2017).

[34]Lefa, E., Rieger, F. M. & Aharonian, F. Formation of Very Hard Gamma-Ray Spectra of Blazars in Leptonic Models. *Astrophys. J.* **740**, 64 (2011).

[35]Böttcher, M., Dermer, C. D. & Finke, J. D. The Hard VHE γ-Ray Emission in High-Redshift TeV Blazars: Comptonization of Cosmic Microwave Background Radiation in an Extended Jet? *Astrophys. J.* **679**, L9 (2008).

[36]Tavecchio, F., Ghisellini, G., Ghirlanda, G., Costamante, L. & Franceschini, A. The hard TeV spectrum of 1ES 0229+200: new clues from Swift. *Mon. Not. R. Astron. Soc.* **399**, L59–L63 (2009).

[37]Tramacere, A., Massaro, E. & Taylor, A. M. Stochastic Acceleration and the Evolution of Spectral Distributions in Synchro-Self-Compton Sources: A Self-consistent Modeling of Blazars' Flares. *Astrophys. J.* **739**, 66 (2011).

[38]Cerruti, M., Zech, A., Boisson, C. & Inoue, S. A hadronic origin for ultra-high-frequency-peaked BL Lac objects. *Mon. Not. R. Astron. Soc.* **448**, 910–927 (2015).

[39]Murase, K., Dermer, C. D., Takami, H. & Migliori, G. Blazars as Ultra-high-energy Cosmic-ray Sources: Implications for TeV Gamma-Ray Observations. *Astrophys. J.* **749**, 63 (2012).

[40]Aharonian, F. A. TeV gamma rays from BL Lac objects due to synchrotron radiation of extremely high energy protons. *New Astron.* **5**, 377–395 (2000).

[41]Essey, W., Kalashev, O. E., Kusenko, A. & Beacom, J. F. Secondary Photons and Neutrinos from Cosmic Rays Produced by Distant Blazars. *Phys. Rev. Lett.* **104**, 141102 (2010).

[42]Taylor, A. M., Vovk, I. & Neronov, A. Extragalactic magnetic fields constraints from simultaneous GeV-TeV observations of blazars. *Astron. Astrophys.* **529**, A144 (2011).

[43]Dzhatdoev, T. A., Khalikov, E. V., Kircheva, A. P. & Lyukshin, A. A. Electromagnetic cascade masquerade: a way to mimic γ-axion-like particle mixing effects in blazar spectra. *Astron. Astrophys.* **603**, A59 (2017).

[44]Tavecchio, F. On the hadronic cascade scenario for extreme BL Lacs. *Mon. Not. R. Astron. Soc.* **438**, 3255–3262 (2014).

[45]Oikonomou, F., Murase, K. & Kotera, K. Synchrotron pair halo and echo emission from blazars in the cosmic web: application to extreme TeV blazars. *Astron. Astrophys.* **568**, A110 (2014).

[46]IceCube Collaboration *et al.* Multimessenger observations of a flaring blazar coincident with high-energy neutrino IceCube-170922A. *Science* **361**, 1378 (2018).

[47]Aartsen, M. G. *et al.* Neutrino emission from the direction of the blazar TXS 0506+056 prior to the IceCube-170922A alert. *Science* **361**, 147–151 (2018).

[48]Gao, S., Fedynitch, A., Winter, W. & Pohl, M. Modelling the coincident observation of a high-energy neutrino and a bright blazar flare. *Nat. Astron.* **3**, 88–92 (2019).

[49]Cerruti, M. *et al.* Leptohadronic single-zone models for the electromagnetic and neutrino emission of TXS 0506+056. *Mon. Not. R. Astron. Soc.* **483**, L12–L16 (2019).

[50]Keivani, A. *et al.* A Multimessenger Picture of the Flaring Blazar TXS 0506+056: Implications for High-energy Neutrino Emission and Cosmic-Ray Acceleration. *Astrophys. J.* **864**, 84 (2018).

[51]Liu, R.-Y. *et al.* Hadronuclear interpretation of a high-energy neutrino event coincident with a blazar flare. *Phys. Rev. D* **99**, 063008 (2019).

[52]Tavecchio, F., Ghisellini, G. & Guetta, D. Structured Jets in BL Lac Objects: Efficient PeV Neutrino Factories? *Astrophys. J.* **793**, L18 (2014).

[53]Padovani, P., Petropoulou, M., Giommi, P. & Resconi, E. A simplified view of blazars: the neutrino background. *Mon. Not. R. Astron. Soc.* **452**, 1877–1887 (2015).

[54]Aab, A. *et al.* Depth of maximum of air-shower profiles at the Pierre Auger Observatory. II. Composition implications. *Phys. Rev. D* **90**, 122006 (2014).

[55]Taylor, A. M., Ahlers, M. & Hooper, D. Indications of negative evolution for the sources of the highest energy cosmic rays. *Phys. Rev. D* **92**, 063011 (2015).

[56]Ajello, M. *et al.* The Cosmic Evolution of Fermi BL Lacertae Objects. *Astrophys. J.* **780**, 73 (2014).

[57]Hillas, A. M. The Origin of Ultra-High-Energy Cosmic Rays. *Annu. Rev. Astron. Astrophys.* **22**, 425–444 (1984).

[58]Taylor, A. M., Ahlers, M. & Aharonian, F. A. Need for a local source of ultrahigh-energy cosmic-ray nuclei. *Phys. Rev. D* **84**, 105007 (2011).

[59]Lemoine, M. & Waxman, E. Anisotropy vs chemical composition at ultra-high energies. *J. Cosmol. Astropart. Phys.* **2009**, 009 (2009).

[60]Alves Batista, R. *et al.* Open questions in cosmic-ray research at ultrahigh energies. *Frontiers Astron. Space Sci.* **6**, 23 (2019).

[61]Guilbert, P. W., Fabian, A. C. & Rees, M. J. Spectral and variability constraints on compact sources. *Mon. Not. R. Astron. Soc.* **205**, 593–603 (1983).

[62]Arons, J. Pulsar Wind Nebulae as Cosmic Pevatrons: A Current Sheet's Tale. *Space Sci. Rev.* **173**, 341–367 (2012).

[63]Hauser, M. G. & Dwek, E. The Cosmic Infrared Background: Measurements and Implications. *Annu. Rev. Astron. Astrophys.* **39**, 249–307 (2001).

[64]Desai, A. *et al.* A GeV-TeV Measurement of the Extragalactic Background Light. *Astrophys. J. Lett.* **874**, L7 (2019).

[65]H.E.S.S. Collaboration. Measurement of the EBL spectral energy distribution using the VHE γ-ray spectra of H.E.S.S. blazars. *Astron. Astrophys.* **606**, A59 (2017).

[66]Acciari, V. A., Ansoldi, S., Antonelli, L. A. *et al.* Measurement of the extragalactic background light using MAGIC and Fermi-LAT gamma-ray observations of blazars up to z = 1. *Mon. Not. R. Astron. Soc.* **486**, 4233–4251 (2019).

[67]Tavecchio, F. & Bonnoli, G. On the detectability of Lorentz invariance violation through anomalies in the multi-TeV γ-ray spectra of blazars. *Astron. Astrophys.* **585**, A25 (2016).

[68]Galanti, G., Tavecchio, F., Roncadelli, M. & Evoli, C. Blazar VHE spectral alterations induced by photon-ALP oscillations. *Mon. Not. R. Astron. Soc.* **487**, 123–132 (2019).

[69]Durrer, R. & Neronov, A. Cosmological magnetic fields: their generation, evolution and observation. *Astron. Astrophys Rev.* **21**, 62 (2013).

[70]Vafin, S., Rafighi, I., Pohl, M. & Niemiec, J. The Electrostatic Instability for Realistic Pair Distributions in Blazar/EBL Cascades. *Astrophys. J.* **857**, 43 (2018).

[71]Ackermann, M. *et al.* The Search for Spatial Extension in High-latitude Sources Detected by the Fermi Large Area Telescope. *Astrophys. J. Suppl.* **237**, 32 (2018).

[72]H.E.S.S. Collaboration. Search for extended γ-ray emission around AGN with H.E.S.S. and Fermi-LAT. *Astron. Astrophys.* **562**, A145 (2014).

[73]Archambault, S. *et al.* Search for Magnetically Broadened Cascade Emission from Blazars with VERITAS. *Astrophys. J.* **835**, 288 (2017).

[74]Liberati, S. Tests of Lorentz invariance: a 2013 update. *Class. Quantum Gravity* **30**, 133001 (2013).

[75]de Angelis, A., Galanti, G. & Roncadelli, M. Relevance of axionlike particles for very-high-energy astrophysics. *Phys. Rev. D* **84**, 105030 (2011).

[76]Lang, R. G., Martínez-Huerta, H. & de Souza, V. Improved limits on Lorentz invariance violation from astrophysical gamma-ray sources. *Phys. Rev. D* **99**, 043015 (2019).

[77]Abdalla, H. *et al.* The 2014 TeV γ-Ray Flare of Mrk 501 Seen with H.E.S.S.: Temporal and Spectral Constraints on Lorentz Invariance Violation. *Astrophys. J.* **870**, 93 (2019).

[78]Abramowski, A. *et al.* Constraints on axionlike particles with H.E.S.S. from the irregularity of the PKS 2155-304 energy spectrum. *Phys. Rev. D* **88**, 102003 (2013).

[79]Merloni, A. *et al.* eROSITA Science Book: Mapping the Structure of the Energetic Universe. *arXiv*:1209.3114 (2012).

[80]Krawczynski, H. *et al.* Astro2020 Science White Paper: Using X-Ray Polarimetry to Probe the Physics of Black Holes and Neutron Stars. *arXiv*:1904.09313 (2019).

[81]de Angelis, A. *et al.* Science with e-ASTROGAM. A space mission for MeV-GeV gamma-ray astrophysics. *J. High Energy Astrop.* **19**, 1–106 (2018).

[82]Cherenkov Telescope Array Consortium *et al.* Science with the Cherenkov Telescope Array. *World Scientific Publishing Co.* **ISBN 9789813270084** (2019).

[83]Bai, X. *et al.* The Large High Altitude Air Shower Observatory (LHAASO) Science White Paper. *arXiv*:1905.02773 (2019).

[84]Albert, A. *et al.* Science Case for a Wide Field-of-View Very-High-Energy Gamma-Ray Observatory in the Southern Hemisphere. *arXiv*:1902.08429 (2019).

[85]Wong, K., Zhdankin, V., Uzdensky, D. A., Werner, G. R. & Begelman, M. C. First-principles demonstration of diffusive particle acceleration in kinetic simulations of relativistic plasma turbulence. *arXiv*:1901.03439 (2019).

[86]Paul, J., Wei, J., Basa, S. & Zhang, S.-N. The Chinese-French SVOM mission for gamma-ray burst studies. *C. R. Phys.* **12**, 298–308 (2011).

[87]Aartsen, M. G. *et al.* IceCube-Gen2: A Vision for the Future of Neutrino Astronomy in Antarctica. *arXiv*:1412.5106 (2014).

[88]Adrián-Martínez, S. *et al.* Letter of intent for KM3NeT 2.0. *J. Phys. G* **43**, 084001 (2016).

[89]The Pierre Auger Collaboration. The Pierre Auger Observatory Upgrade - Preliminary Design Report. *arXiv*:1604.03637 (2016).

[90]Sagawa, H. Telescope Array extension: TAx4. *PoS* **ICRC2015**, 657 (2016).

Source Name	redshift z	X-ray spectrum	γ-ray spectrum	Flux at 1 keV [erg cm^{-2} s^{-1}]	Flux at 100 GeV [erg cm^{-2} s^{-1}]
Mkn 421	0.031	SH	S	$10^{-12} - 10^{-9}$	10^{-10}
Mkn 501	0.034	SH	SH	$10^{-11} - 10^{-10}$	$10^{-10.5}$
1ES 2344+514	0.044	SH	S	$10^{-11.5} - 10^{-10.5}$	10^{-11}
1ES 1959+650	0.048	SH	S	$10^{-11} - 10^{-10}$	10^{-11}
TXS 0210+515	0.049	H	H	10^{-11}	10^{-12}
1ES 2037+521	0.053	H	H?	$10^{-11.5}$	10^{-12}
1ES 1727+502	0.055	HS	SH	10^{-11}	$10^{-11.5}$
PGC 2402248	0.065	H	S?	$10^{-11.5}$	10^{-12}
PKS 0548-322	0.069	H	H	10^{-11}	10^{-12}
RGB J0152+017	0.08	H	S	$10^{-11.5}$	10^{-12}
1ES 1741+196	0.084	H	H	$10^{-11.5}$	$10^{-11.5}$
SHBL J001355.9-185406	0.095	H	S	10^{-11}	10^{-12}
1ES 1312-423	0.105	H	S	10^{-11}	10^{-12}
RGB J0710+591	0.125	H	H	10^{-11}	10^{-12}
1ES 1426+428	0.129	H	SH	10^{-11}	$10^{-11.5}$
RX J1136.5+6737	0.1342	H	S	$10^{-11.5}$	10^{-12}
1ES 0229+200	0.1396	H	H	$10^{-11.5}$	10^{-12}
1ES 1440+122	0.163	H	S	10^{-11}	10^{-12}
H 2356-309	0.165	H	H	10^{-11}	10^{-12}
1ES 1218+304	0.182	HS	H	10^{-11}	10^{-11}
1ES 1101-232	0.186	HS	H	10^{-11}	$10^{-11.5}$
1ES 0347-121	0.188	H	H	10^{-11}	10^{-12}
RBS 0723	0.198	H	S	$10^{-11.5}$	10^{-12}
1ES 0414+009	0.287	S	H	10^{-11}	$10^{-11.5}$

Table 1. Main properties of the TeV-detected extreme blazars with firm redshift. H = hard spectrum (extreme behaviour); S = soft spectrum; HS = mostly hard spectrum, sometimes soft; SH = mostly soft spectrum, becoming hard when flaring. Fluxes at 1 keV and 100 GeV are rounded to half a dex.